Polymer 50 (2009) 4535–4542

Contents lists available at ScienceDirect

Polymer

journal homepage: www.elsevier.com/locate/polymer

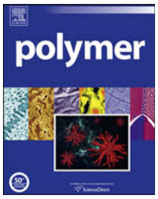

Water–Polymer interactions in PVME hydrogels – Raman spectroscopy studies

M. Pastorczak*, M. Kozanecki, J. Ulanski

Department of Molecular Physics, Technical University of Lodz, Zeromskiego 116, 90-924 Lodz, Poland

A R T I C L E I N F O

Article history:
Received 4 May 2009
Received in revised form
27 July 2009
Accepted 28 July 2009
Available online 3 August 2009

Keywords:
Thermo-responsive hydrogels
Intermolecular interactions
Raman spectroscopy

A B S T R A C T

Raman spectroscopy was used to investigate molecular interactions and structure of water in PVME hydrogels of various crosslinking degrees. Analysis of polymer ν(CH_3) and ν(CH_2) stretching vibrations has allowed to monitor the changes of hydrophilic and hydrophobic polymer–water interactions in a course of water deswelling and volume phase transition. Formation of water–polymer hydrogen bonds has appeared to influence directly supramolecular structure of the absorbed water. It was found that the polymer network density determines an availability of the hydrophilic sites to water molecules and also influences the kinetics of volume phase transition of the hydrogels. Activation energy of the volume phase transition in the investigated systems was estimated to be ca.88 kJ/mol.

1. Introduction

Poly(vinyl methyl ether) (PVME) is an amorphous polymer which can act as a perfect component of model systems for studies of an intermolecular interactions and molecular dynamics in polymer–water mixtures (solutions, hydrogels). The instable balance between hydrophilic and hydrophobic sites of this polymer results in the lower critical solution temperature (LCST) of the PVME/water mixtures which is particularly interesting from the point of view of possible applications. In the case of a hydrogel, the LCST manifests in volume phase transition (VPT) during which water is rapidly pulled out from collapsing polymer network. Because the LCST temperature of the PVME hydrogels, $T_{LCST} = 37\ ^{\circ}C$, is located in the vicinity of the body temperature of mammals, there are expected wide applications of PVME hydrogels in medicine and pharmacy [1]. The additional advantage of the PVME is that it can be radiationally crosslinked (by mean of electron-beam or γ-irradiation) [2,3]. Such way of formation of the hydrogels gives many benefits as it was documented by Rosiak and co-workers [2,4]. The most important is obviously one-step synthesis and simultaneous sterilisation of the product which allows for establishing simple and “compact” technology. Moreover, thanks to lack of any additives (e.g. initiators, crosslinkers) required for chemical crosslinkage, the process is environmentally friendly, and the final product is not contaminated by ballast materials or the residual toxic initiators. It is also interesting to notice the successful attempts of usage of PVME hydrogels for removal of organic impurities from water solutions [5].

Up to now most of studies concerning PVME have been devoted to linear polymer and its aqueous solutions. The substantial works performed by Maeda [6–8] with use of vibrational spectroscopy have shown that the positions of symmetric as well as the antisymmetric stretching vibrations of CH_3 groups (ν(CH_3)) in PVME shift to blue upon dilution. Good correlation of these shifts with the red shift of C–O stretching vibrations (ν(C–O)) against the water concentration proves that the positions of both modes reflect the hydration degree of polymer chain. Maeda has shown that this method allows also monitoring the LCST of the PVME solution. Hanykova et al. investigated the VPT in PVME gels as well as the LCST in the solutions of uncrosslinked polymer by ^{1}H NMR [9,10]. It was observed that both the phase separation in solution and the collapse of gels of crosslinked PVME resulted in broadening of NMR lines of a major part of PVME units due to a formation of globular-like structures. Detailed investigations supported by theoretical considerations have shown that the PVME/water solutions exhibit unusual, the so called type III, demixing behaviour [11,12]. This behaviour is characterised by presence of two off-zero limiting critical concentrations – the miscibility gap is bimodal at large average molar mass of the polymer [11].

Another interesting phenomena in the PVME/water systems occur at sub-zero temperatures because the glass transition temperature of neat polymer ($T_g = -25\ ^{\circ}C$) is lower than the melting point of water. Water crystallisation leads to formation of concentrated solution of PVME confined between water crystals, what can result in untypical molecular dynamics [13–15] as well as in specific changes in molecular interactions. Extended studies with

---

* Corresponding author. Tel.: +48 426313205; fax: +48 426313218.
E-mail address: marcin.pastorczak@p.lodz.pl (M. Pastorczak).

0032-3861/$ – see front matter © 2009 Elsevier Ltd. All rights reserved.
doi:10.1016/j.polymer.2009.07.048

use of Temperature Modulated Differential Scanning Calorimetry (TMDSC) and complementary techniques (IR, turbidimetry) on aqueous solutions of PVME in broad range of temperatures were conducted in the group from *Polymer Research Division, Katholieke Universiteit Leuven* [16–18]. In the early works of this group phase transitions were studied also in a densely crosslinked (with use of dose 80 kGy of X-radiation) hydrogel sample [16].

Although many efforts were made to understand properties and structure of aqueous solutions of PVME, the hydrogels prepared from this polymer are rather poorly investigated. Moreover, high equilibrium swelling degrees (SD–see formula (1)) reached by chemically crosslinked PVME hydrogels (i.e. low polymer and high water fraction) is a source of various experimental difficulties, e.g.: domination of ionic conductivity in dielectric spectroscopy, very high absorbance by water in IR spectroscopy, etc. Raman spectroscopy is thus an advantageous tool for studying such systems. Firstly, Raman activity of OH stretching multimode band being relatively low comparing to IR absorption, makes possible successful analysis of structure of imbibed water [19–21]. The Raman activity of bands related to stretching vibrations of CH_x groups is rather high in comparison to the to OH stretching, thus even low concentration of polymer may be detected, what together with high spectral resolution (ca. 0.5 cm^{-1}) of Raman spectroscopy enables precise analysis of particular bands shifts. Therefore, both hydrophilic and hydrophobic water–polymer interactions may be with this technique monitored.

In this work, Raman spectroscopy was employed to investigate water–water and water–polymer interactions in the PVME hydrogels of various crosslinking degrees. Changes of the interactions were studied vs. gel's swelling degree as well vs. temperature in the range 25–50 °C.

2. Experimental

2.1. Materials – hydrogel preparation

Poly (vinyl methyl ether) (PVME) was purchased from Aldrich Chemical Co. as a 50 wt.% aqueous solution. Its molecular weight, determined by static light scattering in water, was estimated as $M_w = 65{,}000$ g/mol. The polymer was processed without any further purification. PVME was dissolved in water by overnight stirring at room temperature (RT). Solutions were prepared with water purified by distillation and subsequent passing through the Nanopure II system (Barnstead, final specific resistance >17 MΩ cm).

The hydrogel samples were prepared in the laboratory headed by Janusz Rosiak from Technical University of Lodz by irradiation of 10% (w/v) PVME solutions (ampoules volume: 2 mL) in accelerator ELU-6E delivering pulses of 6 MeV electrons. Polymer solutions were treated with different doses of electron-beam irradiation: 13 kGy (sample PVME-13), 15 kGy (PVME-15), 18 kGy (PVME-18), 22 kGy (PVME-22), 35 kGy (PVME-35), 42 kGy (PVME-42) and 65 kGy (PVME-65) what resulted in various crosslinking degrees of polymer. Detailed description of irradiation procedures as well as the sol-gel analysis of synthesised networks was published elsewhere [22,23].

2.2. Experimental method

The Raman spectra were acquired with use of JobinYvon T64000 triple-gratings spectrometer equipped with the Olympus BX40 confocal microscope. Ar-ion laser (LEXEL) lines (457.9, 488.0 and 514.5 nm) were used for samples excitation. Different laser lines were selected to avoid fluorescence of the samples which would otherwise mask the Raman bands. Laser power (4–6 mW at a sample) and time of a single measurement (240–360 s) were adjusted to obtain high quality Raman spectra and to avoid overheating of the samples.

The Raman analyses of water–polymer interactions for different SD of the hydrogels were performed during a dynamic, spontaneous deswelling in air. Swelling degree is defined as:

$$SD = m_W/m_P[g/g] \tag{1}$$

where m_W is a mass of water absorbed by the polymer and m_P a mass of dry polymer. Raman spectra were acquired with the microscope objective (×50, N.A. = 0.5) focused 30–40 μm below a sample surface. After each measurement the hydrogel sample was weighted in order to determine its SD. Initial weights of samples were 50–150 mg. For each sample two series of measurements were performed.

For studies of molecular interactions around the LCST temperature of PVME (25–50 °C), the gel samples were placed in a hot stage (SEMIC) mounted under the microscope objective. Stabilisation of a temperature (±0.01 °C) was secured by Shimaden FP93 temperature controller. Before each measurement a sample was conditioned for 5–6 min to reach the set temperature. Between the measurements mass of the samples was controlled.

2.3. Mathematical analysis of experimental data

Baseline correction was performed for all spectra with use of the 3rd order polynomial. Subsequently the spectra were area normalised to be directly comparable. For the purpose of 2nd derivative calculation as well as data presentation some spectra were smoothed with FFT filter. Peaks were fitted with use of Gauss + Lorentz Area deconvolution procedure (PeakFit v.4, Jandel).

3. Results and discussion

3.1. Intermolecular interactions vs. hydrogel swelling degree

Fig. 1 presents normalised Raman spectra of water, of neat linear PVME and of hydrogel PVME-42 in equilibrium SD. In the low frequency part of the spectra (2700–3100 cm^{-1}) there are well visible CH_x stretching vibrations of PVME; in the high frequency part one can see broad multimode band connected with OH stretching of liquid water. Shapes of the water stretching bands in the equilibrium swollen hydrogel and those of the distilled water, do not differ. This observation indicates that in the hydrogel in equilibrium SD, the not disturbed (bulk) water dominates.

As it was shown in Maeda's work [6] concerning IR studies of PVME solutions, bands at ca. 2822 cm^{-1} and 2971 cm^{-1} (for neat PVME) are related to symmetric ($\nu_s(CH_3)$) and antisymmetric ($\nu_{as}(CH_3)$) C–H stretching of CH_3 respectively, and their positions reflect a degree of hydration of the $-OCH_3$ groups. The assignment of the CH_x groups vibrations to the strongly overlapped bands (at ca. 2893, 2922 and 2946 cm^{-1}) is uncertain in a view of existent literature [6,7,24]. However, it is well known that in contrast to the symmetric modes, the antisymmetric ones are insensitive to the polarisation of excitation light. Therefore, for appropriate assignment of the overlapped modes the polarisation spectra of an exemplary sample (PVME-42) were collected (Fig. 2). Contrary to the bands at 2893 and at ca. 3000 cm^{-1} which reveal only small loss in intensity for perpendicular polarisation, the relative intensities of the bands at 2842 and 2922 cm^{-1} decrease significantly. There is also visible a decrease in relative intensity of the band at ca. 2951 cm^{-1}. Yet, as can be deduced from the comparison of intensities of the bands 2922 and 2951 cm^{-1} in dry and swollen polymer

(Fig. 1), this effect comes from decrease of band 2922 cm^{-1} which has substantial contribution to the latter one. Thus, it can be claimed that the bands 2842 and 2922 cm^{-1} are related to the symmetric modes, while the bands at 2893, 2951 and 2998 cm^{-1} can be assigned to the antisymmetric ones as proposed in Table 1. It is consistent also with the fundamental rule stating that a symmetric mode of a particular vibration has always higher energy than an antisymmetric one.

In order to study an influence of water content on the molecular interactions in the gels, the Raman measurements were performed during the deswelling process. In Fig. 3 the $\nu_s(CH_3)$ band positions are plotted vs. the SD for the samples: PVME-13, PVME-22, PVME-65. For all the samples the band positions are constant for SD higher than 3, while for lower SD the bands abruptly shift to lower wavenumbers. The shift of the $\nu_s(CH_3)$ band for SD $\leq$ 3 for all the samples follows the exponential decay. The “plateau” seen for SD $\geq$ 3 indicates that the –OCH_3 groups of the polymer are totally hydrated and the “extra” swollen water are localised in the interstitial regions. One can see also, that the “plateau” positions of the $\nu_s(CH_3)$ band for high SDs are different for different samples. The mean values against dose applied in sample crosslinking process are shown in an inset in Fig. 3. The highest values (i.e. the strongest shift) are found for the samples PVME-13 and PVME-15 (2844 cm^{-1}), and the lowest for the PVME-65 (2840 cm^{-1}). Because the position of the $\nu_s(CH_3)$ band is sensitive to hydration of the –OCH_3 groups, it can be concluded that for the high SDs, these groups are less hydrated in the strongly crosslinked polymer then in the loosely crosslinked ones. This effect can be correlated with the average distances between the crosslinks for different samples. From the sol-gel analysis the average molecular weight of chains between the crosslinks (M_C) was estimated to be ca. 1065 Da for the sample PVME-13 and ca. 185 Da for the sample PVME-65 [23]. Taking into account that a molecular weight of the PVME monomer unit is 58 Da, one can estimate that an average chain between crosslinks in PVME-13 contains over 18 monomer units while in PVME-65 only 3–4 units. Consequently, hydrophilic groups in the latter case are much less accessible to water molecules.

Analysis of interactions of the CH and CH_2 groups was more difficult due to overlapping of the bands related to their stretching modes (see Table 1 and the spectral region 2860–2960 cm^{-1} in Fig. 4a). The second derivatives of smoothed spectra were calculated and the positions of their local minima indicate that the positions of the bands at 2893, 2922 and 2951 cm^{-1} do not depend on the swelling degree. The water–polymer interactions are thus manifested only by the changes of intensities of particular bands. To determine the relationship between these intensities and the SD, the difference spectra of the gels to the spectrum of dry polymer were prepared. Each spectrum was previously normalised to its integral intensity in the region 2600–3050 cm^{-1}. The difference spectra (Fig. 4b shows a set of spectra for PVME-22 as an exemplary one) reveal that with increase in concentration of water in the system the intensity ratio of symmetric (2922 cm^{-1}) and antisymmetric (2946 cm^{-1}) CH_2 stretching bands changes. The lack of direct compensation of seen increase in intensity of $\nu_{as}(CH_2)$ band

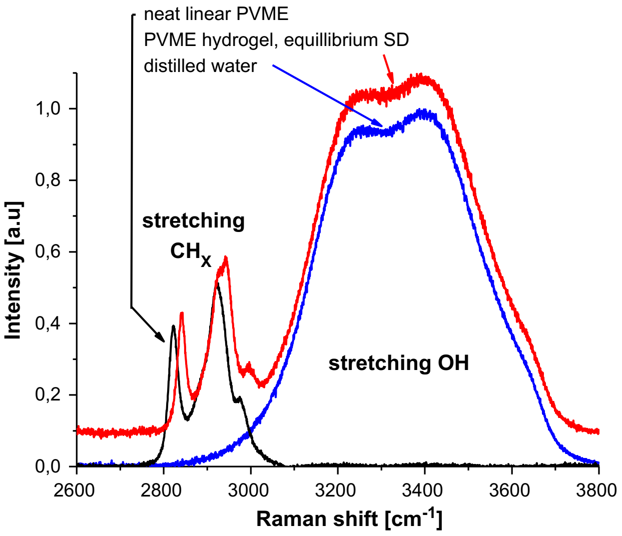

Fig. 1. Raman spectra of neat linear PVME (black), PVME-42 hydrogel in equilibrium swelling degree (red) and distilled water (blue) in the region 2600–3800 cm^{-1}. Water and hydrogel spectra are normalised to the maxima of intensity (at ca. 3410 cm^{-1}). Neat PVME spectrum was scaled so as to be comparable in intensity with polymer bands in hydrogel spectrum. Hydrogel spectrum is shifted up vertically for transparency of the figure.

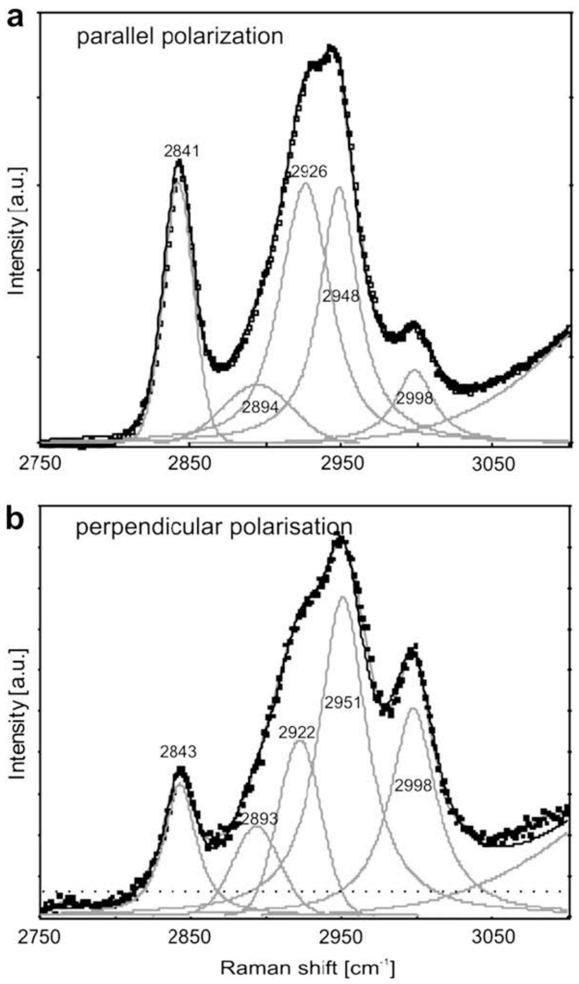

Fig. 2. Raman polarisation spectra of hydrogel PVME-42 for (a) parallel (x(y,y)z) and (b) perpendicular (x(y,x)z) configuration. Results of deconvolution are marked with grey lines. Position of maxima of particular peaks derived by the deconvolution are marked on the spectra.

Table 1
Assignment of vibrational modes to Raman bands observed in the spectral region 2600–3050 cm^{-1}.

Position of centre of band [cm^{-1}]	2842	2893	2922	2951	2998
Assignment	Symmetric stretching of CH_3 $(\nu_s)CH_3$	Stretching of CH $(\nu_s)CH$	Symmetric stretching of CH_2	Antisymmetric stretching of CH_2 $(\nu_{as})CH_2$	Antisymmetric stretching of CH_2 $(\nu_{as})CH_3$

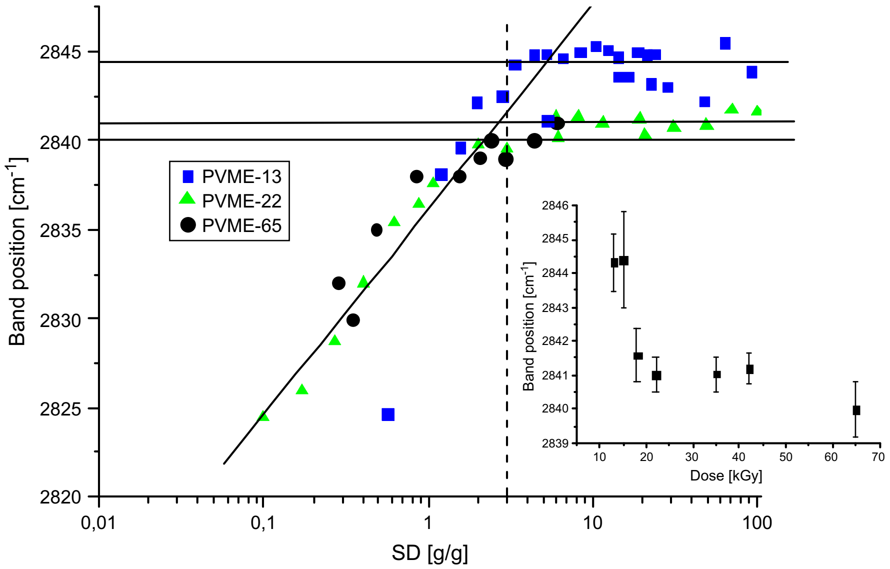

Fig. 3. Plot of the $\nu_s(CH_3)$ band position against the swelling degree for the gels: PVME-13 (squares), PVME-22 (triangles) and PVME-65 (circles) measured at room temperature. Horizontal lines mark the average wavelengths of the "plateau" part of the graph for each hydrogel. The slope of the line in the left part of the graph was averaged over the results obtained for all studied samples. Inset – plot of the mean values of the "plateau" against the dose applied for the crosslinking.

by a decrease in intensity of band $\nu_s(CH_2)$ may be due to different Raman activity of both modes. Changes of intensity of these two modes vs. SD for the sample PVME-22 are presented in Fig. 5 as a difference between the intensity at 2946 cm^{-1} and the intensity at 2922 cm^{-1} (the intensities I_{2946} and I_{2922} are taken from the difference spectra). It is evident that this dependence exactly follows the dependencies of symmetric and antisymmetric CH_3 modes against SD. The possible explanation is that the water molecules, bounded to oxygen atoms in methoxy groups, interact hydrophobically with CH_2 groups and thus disturb the symmetry of their vibrations. Moreover, it suggests that the hydrophilic interactions OCH_3–H_2O are balanced by the hydrophobic interactions CH_2–H_2O. Such balance of the hydrophilic/hydrophobic interactions in water–PVME system determines its properties in temperatures lower than 37 °C.

The CH stretching band (2893 cm^{-1}) in the gels is less intensive comparing to neat PVME what is manifested by negative values of

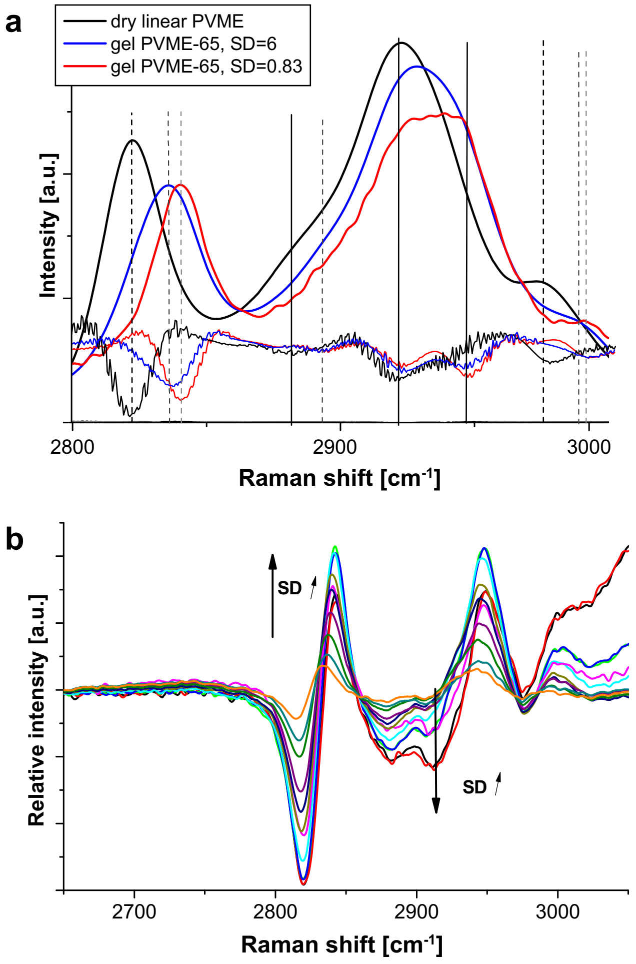

Fig. 4. (a) – Raman spectra of the neat linear PVME (black) and of the crosslinked hydrogel PVME-65 with SD = 6 (blue) and SD = 0.83 (red) in the region 2800–3000 cm^{-1} and second derivatives over the spectra; minima of the second derivatives are marked with vertical lines; (b) difference spectra of the PVME-22 hydrogel for various SD related to the spectrum of the dry linear PVME. Main changes in intensity with SD are marked with arrows. Notice, that the x-scales in sections 4a) and 4b) are different for better clarity of presented differences in particular spectra.

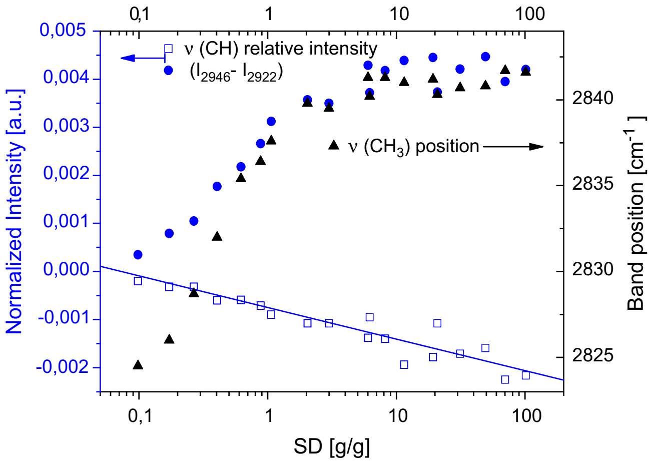

Fig. 5. Changes of spectral parameters related to the modes ν(CH), $\nu(CH_2)$ and $\nu(CH_3)$ against SD for the sample PVME-22. Right y-axis denotes wavelength of maximum of the band $\nu_s(CH_3)$ (triangles). Left y-axis denotes changes in relative intensities of the band ν(CH) (squares) and relative intensity differences between the modes $\nu_s(CH_2)$ and $\nu_{as}(CH_2)$ (circles); for more details see text.

its intensity for swollen gels in the difference spectra. One can see that intensity of the 2893 cm^{-1} band increases monotonically with decreasing SD. Such tendency, different to those for the CH_2 and CH_3 stretching bands, is characteristic for all studied PVME gels. An explanation for the observed tendency one can deduce from Fig. 6, where the intensity of the 2893 cm^{-1} band and polymer fraction are plotted vs. time of the desorption process for the sample PVME-22. It is clear that these two dependencies are strictly correlated, what indicates that the intensity of the ν(CH) mode directly relates to the polymer fraction in a sample. Hence, one can use it to determine concentration of the polymer in the aqueous solution. In the same time positions of the symmetric as well as the antisymmetric CH_3 stretching modes may be utilised to conclude about a degree of local hydration of methoxy groups.

Raman spectroscopy allows also for *in-situ* monitoring of changes in water structure during the desorption processes. As a measure of dynamic structure of water the I_{3400}/I_{3200} parameter is commonly used [19,25], however it sets aside all changes in H-bonded network reflected in high frequency modes (around 3500 and 3600 cm^{-1}) of the broad multimode OH stretching band. Moreover, it was previously found that the I_{3400}/I_{3200} ratio depends on the excitation wavelength owing to the Raman resonance effect [26]. For that reason the difference spectra of the water in the hydrogels related to the spectrum of the distilled water (obtained for the same excitation wavelength) were prepared (see Fig. 7) and following parameter was calculated:

$$S = I_{3400} + I_{3500} + I_{3600} - I_{3200} \tag{2}$$

where: I_{3200}, I_{3400}, I_{3500} and I_{3600} are relative intensities at 3200, 3400, 3500 and 3600 cm^{-1} respectively, taken from the difference spectra. Such studies were performed for all the samples and Fig. 8 presents the evolution of both ratio of integrated intensity of the bands at 3400 and 3200 cm^{-1} (I_{3400}/I_{3200}) and S with the swelling degree for the sample PVME-22 (please note the additional left axis). Parameter S reflects similar dependence on SD as the I_{3400}/I_{3200} ratio, however it is less scattered.

To make the analysis easier the $\nu_s(CH_3) = f(SD)$ dependence is plotted in the same graph (right axis). As one can see the changes of S are similar to the changes of position of the $\nu_s(CH_3)$ band. For swelling degrees above ca. 1 the S parameter has constant value c.a. 0.5×10^{-5} what is slightly above 0, characteristic for distilled water. This value corresponds to I_{3400}/I_{3200} ratio equal 1.02 (I_{3400}/I_{3200} for distilled water is ca. 0.84). For lower SDs value of S parameter increases simultaneously with the shifting of the band $\nu_s(CH_3)$. Also in the hydrogel samples with other crosslinking degrees the structure of water changes with SD similarly to described above.

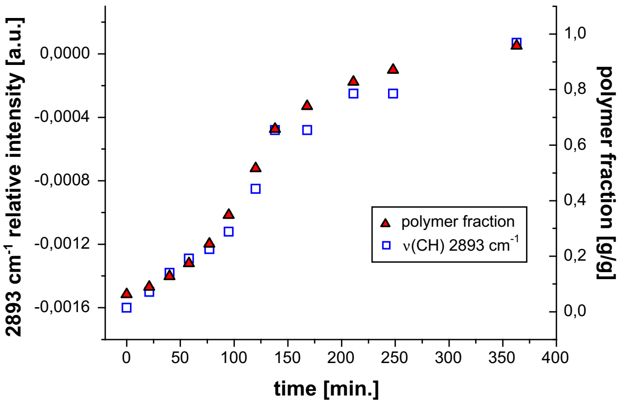

Fig. 6. Changes in polymer fraction in the hydrogel PVME-22 (triangles, right *y*-axis) vs. time of desorption process with superimposed changes in relative intensity of band ν(CH) (squares, left *y*-axis).

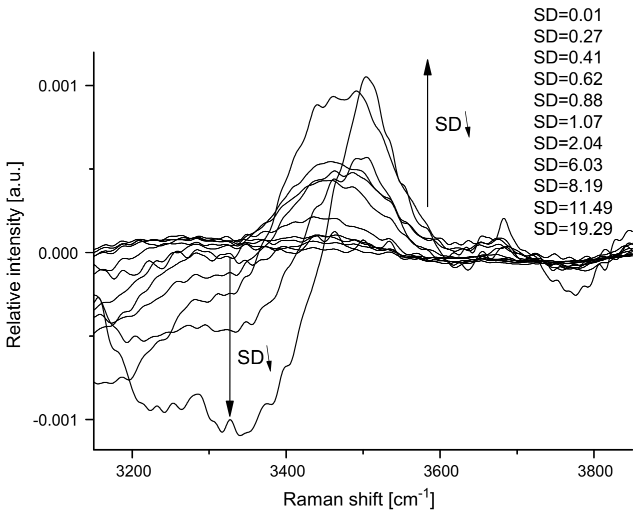

Fig. 7. Difference spectra of water in the hydrogel PVME-22 with various SD related to the spectrum of distilled water (obtained for the excitation wavelength 514.5 nm). Changes in relative intensities with SD are marked with arrows.

These results demonstrate that the water–polymer interactions affect the network of the hydrogen bonds constituted by water molecules. The "plateau" of S = f(SD) reflects the situation where majority of water molecules are linked to molecules of the same type via H-bonds (i.e. bulk water predominates). The increase of the S parameter reflects the increase of a relative fraction of the water molecules linked to the polymer chain.

3.2. Intermolecular interactions – LCST transition

Assuming that the position of the $\nu_s(CH_3)$ band in Raman spectra reflects the degree of hydration of the $–OCH_3$ groups, it should be possible to follow kinetics of volume phase transition by monitoring the shift of this band with increasing temperature. Evolutions of the $\nu_s(CH_3)$ band were monitored for all the samples, Fig. 9 shows representative spectra for the sample PVME-22 at 24 °C and at 45 °C (after very quick heating, so one can assume that an amount of water in a system was constant). The difference spectrum shows shifts of the bands at 2842 cm^{-1} and at 2998 cm^{-1}

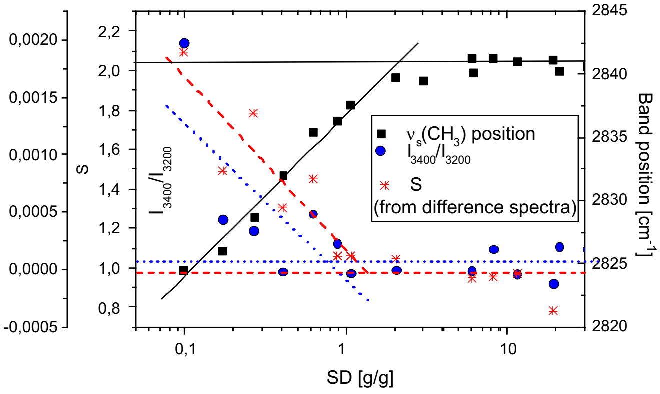

Fig. 8. Position of the band $\nu(CH_3)$ (squares, right *y*-axis) against SD of exemplary hydrogel. Changes in structure of imbibed water are represented as parameter I_{3400}/I_{3200} (circles, 1st left *y*-axis) and parameter S (stars, 2nd left *y*-axis). Solid trend lines are related to the $\nu(CH_3)$, dotted lines to the parameter I_{3400}/I_{3200} and dashed lines to the parameter S.

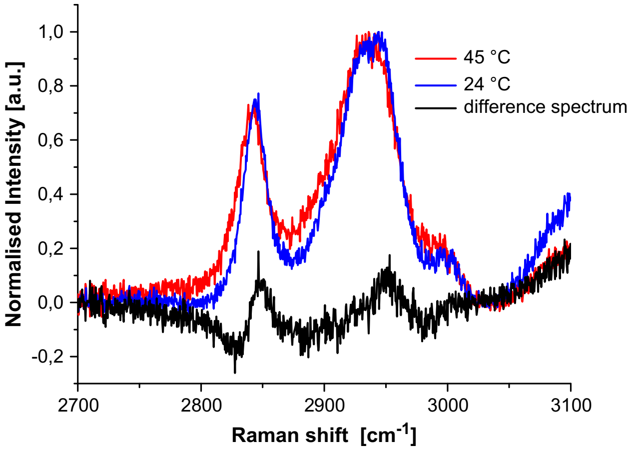

Fig. 9. Spectrum of the sample PVME-22 at 24 °C (blue) and after abrupt heating up to 45 °C (red); black line represents the difference spectrum (spectrum at 24 °C minus spectrum at 45 °C).

related to the symmetric and antisymmetric stretching of the CH_3 groups, respectively and an increase in intensity of the band at 2951 cm^{-1} related to the antisymmetric stretching of CH_2 groups when the temperature exceeds LCST. Because of nearly constant weight of the sample in both measurements one can conclude that the observed changes in bands parameters are not related to the water evaporation during heating but to the modification of the water–polymer interactions. Fig. 10 presents relation between the position of the band $\nu_s(CH_3)$ and the temperature for several samples. Bands $\nu_{as}(CH_3)$ (not shown here) exhibit the same tendency. For all investigated hydrogels one can observe a shift of the bands for temperatures related to VPT. However, a slope connected with VPT is steeper for the samples PVME-15 and PVME-18, and smoother for the samples PVME-50 and PVME-65, i.e. with higher degree of crosslinking. High crosslinking degree can affect the transition in two ways. First of all coil-to-globule transition of PVME chains is more difficult in a denser (i.e. stiffer) network which in consequence reacts slower on temperature changes. Secondly, the crosslinking process may reduce a number of hydrophilic methoxy groups making a gel sample more hydrophobic.

One can see in Fig. 9 that heating the PVME hydrogel over the LCST results also in a change of the integral intensities ratios of the $\nu_s(CH_2)$ to $\nu_{as}(CH_2)$, (similar to that described in Section 3.1), as a result of the hydrophobic water–polymer interactions. According to the Raman scattering theory this ratio reflects distribution of the CH_2 groups of PVME which undergo symmetric and antisymmetric stretch vibrations. As it was pointed out by Walrafen [27], presentation of such redistribution of the vibronic states against inversed temperature may be used for evaluation of an activation energy of the process, from Arrhenius-type equation:

$$\frac{I\nu_s(CH_2)}{I\nu_{as}(CH_2)} = Ae^{\frac{-E_a}{RT}} \qquad (3)$$

where $I\nu_s(CH_2)$ and $I\nu_{as}(CH_2)$ are integral intensities of symmetric and antisymmetric CH_2 stretch vibrations, A – a constant, E_a – the apparent activation energy of the process and R – the gas constant.

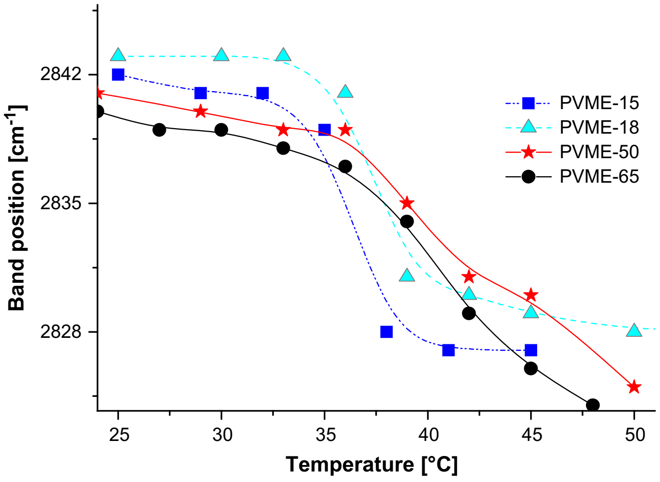

Fig. 10. Dependence of position of the band $\nu_s(CH_3)$ on the temperature for the samples: PVME-15 (squares), PVME-18 (triangles), PVME-50 (stars) and PVME-65 (circles). Lines are for eye guidance.

Fig. 11 shows natural logarithm of the ratio of $I\nu_s(CH_2)$ to $I\nu_{as}(CH_2)$ vs. inversed temperature for the samples PVME-22 and PVME-65. For both systems the experimental points follow a linear regression only between 30 °C and 45 °C. This range fits well the temperature range of the VPT transition observed in the studied hydrogels. The activation energy determined for this temperature range is 88 ± 2 kJ/mol ($R^2 = 0.998$) and 88 ± 5.1 kJ/mol ($R^2 = 0.983$) for the PVME-22 and the PVME-65 systems, respectively. Interestingly, Zhu and Napper [28] reported similar activation energy (80 kJ/mol) for extended-to-loopily transition of the poly(*N*-isopropylacrylamide) (PNIPAM) absorbed from water solution onto a solid substrate. Their results were derived from dynamic light scattering measurements of the solution in different temperatures. The extended-to-loopily absorbed transition of PNIPAM is regarded as similar to the coil-to-globule transition observed in systems in which PNIPAM chains are anchored to the particle surface [29]. Processes observed in the PVME hydrogels and in the PNIPAM aqueous solution reveal similar activation energy probably because they both consist of two major steps-collapse of polymer chain and desorption of water molecules. What is more, in both cases polymer chains are anchored either to the crosslinking centres (PVME) or the to the solid substrate (PNIPAM). Differences in the chemical structure seem to have a minor influence on the activation energy of this process.

It was found also that the VPT transition influences the structure of water in the gels. Fig. 12 presents difference Raman spectra of water in the sample PVME-22 related to the spectrum of distilled water in adequate temperature (all the spectra were obtained for the same excitation wavelength). As one can see the spectra acquired in temperatures 24–30 °C reveal practically no difference

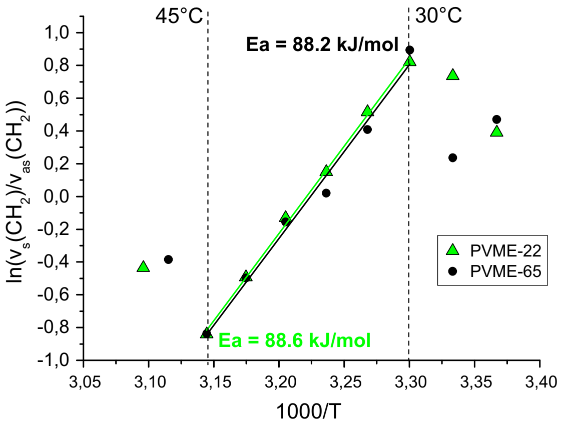

Fig. 11. Natural logarithm of a ratio of intensities of the $\nu_s(CH_2)$ to $\nu_{as}(CH_2)$ against inversed temperature for the samples PVME-22 and PVME-65. Dotted lines indicate temperature range with linear dependence of the analysed value. Solid lines present linear fitting of the experimental points between 30° and 45 °C.

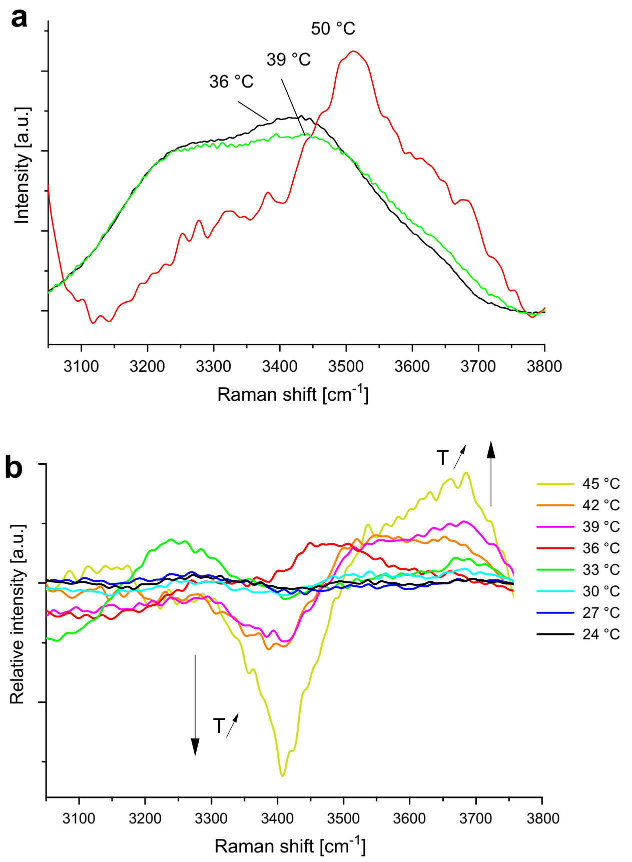

Fig. 12. (a) The Raman spectra of the PVME-22 hydrogel in the OH stretching range of water at 36 °C (black), 39 °C (green) and 50 °C (red); (b) the difference spectra of sample PVME-22 to spectra of distilled water measured in the same temperature ranged from 24° to 45 °C. Arrows indicate changes in relative intensity with temperature increase.

between the gel and distilled water what reflects the fact that the H-bond network of water molecules is similar in both samples. The spectra taken at 33 °C and 36 °C reveal small and non-systematic differences, probably because they are acquired just at the beginning of the volume phase transition. For higher temperatures the differences between water in gels and distilled water increase. The spectra of water in gel obtained in the temperatures 39–45 °C have lower intensity around 3400 cm^{-1} than the spectra for distilled water in the same temperatures. From this finding one can infer that above LCST of the polymer the structure of water present in the gel is less disturbed than in the distilled water in the same temperature. This should be correlated with the fact, that above VPT hydrophobic interactions prevail. Consequently, it can be deduced that predominance of the water–polymer interaction of the hydrophobic type is a water structure-making factor. In the difference spectrum it can be noticed also with increasing temperature an increase of the OH bands intensity in the region at ca. 3550–3750 cm^{-1}. Water bands appearing in this spectral region are usually assigned to free (non H-bonded) OH oscillators or OH oscillators of water molecules present at a hydrophobic surface [30]. This observation indicates presence of the fraction of water molecules which are caged in the interstitial regions due to polymer network collapsing (above LCST).

To summarise, below LCST of the polymer the average structure of water in gel is similar to the structure of distilled water in the same temperature. Above the critical solution temperature, however, the H-bonds network of residual water in hydrogels is much less disturbed than that of bulk water in the same temperature. Hydrophobic (in the temperature above LCST) PVME network acts therefore as a “structure-making” agent.

4. Conclusions

Analyses of stretching modes in polymer (CH_x groups) and in water (OH groups) observed in PVME hydrogels spectra allow us to conclude that:

1) Formation of water–polymer hydrogen bonds (seen as shifts of the $\nu_s(CH_3)$ bands) directly influences supramolecular structure of water absorbed by the hydrogel. However, for high swelling degree (for $SD > 3–4$, i.e. for ca. 10–13 water molecules per monomer unit) the additionally absorbed water does not interact with the polymer network.
2) Hydrophobic water–polymer interactions, which manifest in perturbation of symmetry of the $\nu(CH_2)$ vibrations, are in equilibrium with hydrophilic interactions over wide range of swelling degrees at room temperature.
3) Crosslinking density of the polymer network influences the availability of the hydrophilic sites to water molecules what reduces the equilibrium SD of the hydrogel. Moreover, conformational changes are more difficult in dense rigid network and consequently the volume phase transition is smoother in gels crosslinked with high irradiation dose. Collapse of the polymer network over LCST results in trapping of some quantity of water, which is (probably due to hydrophobic water–polymer interactions) more structured comparing to distilled water in the same temperature.

Acknowledgements

Authors thanks Prof. J.M. Rosiak and Dr S. Kadlubowski for granting the samples originally elaborated by them for our studies. This project was supported by Polish Ministry of Education and Science (grant no. 3TO8E 027 30) and by EU project DIELPOL No. MTKD-CT-2005-029670.

References

[1] Gil ES, Hudson SM. Prog Polym Sci 2004;29:1173–222.
[2] Janik I, Ulanski P, Rosiak JM. Pulse radiolysis of poly(vinyl methyl ether) in aqueous solution. Formation and structure of primary radicals. Elsevier Science; 1999.
[3] Arndt K-F, Schmidt T, Menge H. Macromol Symp 2001;164:313–22.
[4] Rosiak JM, Ulański P, Pajewski A, Yoshi F, Makuuchi K. Radiat Phys Chem 1995;46(2):161–8.
[5] Yamagiwa K, Katoh M, Yoshida M, Ohkawa A, Ichijo A. Wat Sci Technol 1997;35(7):213–8.
[6] Maeda Y. Langmuir 2001;17:1737–42.
[7] Maeda Y, Yamamoto H, Ikeda I. Langmuir 2004;20:7339–41.
[8] Maeda Y, Mochiduki H, Yamamoto H, Nishimura Y, Ikeda I. Langmuir 2003;19:10357–60.
[9] Hanykova L, Spevacek J, Ilavsky M. Polymer 2001;42:8607–12.
[10] Hanykova L, Labuta J, Spevacek J. Polymer 2006;47:6107–16.
[11] Schafer-Soenen H, Moerkerke R, Berghmans H, Koningsveld R, Dusek K, Solc K. Macromolecules 1997;30:410–6.
[12] Pyda M, Van Durme K, Wunderlich B, Van Mele B. NATAS Notes 2005;47(4):7–13.
[13] Shinyashiki N, Shimomura M, Ushiyama T, Miyagawa T, Yagihara SJ. Phys Chem B 2007;111:10079–87.
[14] Shinyashiki N, Matsumura Y, Mashimo S, Yagihara SJ. Chem Phys 1996;104(17):6877–80.
[15] Cerveny S, Colmenero J, Alegria A. Macromolecules 2005;38:7056–63.
[16] Meeussen F, Bauwens Y, Moerkerke R, Nies E, Berghmans H. Polymer 2000;41:3737–43.
[17] Van Durme K, Loozen E, Nies E, VanMele B. Macromolecules 2005;38:10234–43.
[18] Loozen E, Van Durme K, Nies E, Van Mele B, Berghmans H. Polymer 2006;47:7034–42.
[19] Maeda Y, Kitano H. Spectrochim Acta Part A 1995;51:2433–46.
[20] Tominaga Y, Fujiwara A, Amo Y. Fluid Phase Equilib 1998;144:323–30.
[21] Walrafen GE. J Chem Phys 1967;47:114.

[22] Janik I, Rosiak JM. Radiat Phys Chem 2002;63:529–32.

[23] Pastorczak M, Kadlubowski S, Okrasa L, Kozanecki M, Boiteux G, Rosiak J, et al. J Non-Cryst Solids 2007;353(47–51):4536–40.

[24] Guo Y, Peng Y, Wu P. J Mol Struc 2008;875:486–92.

[25] Joachimiak A, Halamus T, Wojciechowski P, Ulanski J. Macromol Chem Phys 2005;206(1):59–65.

[26] Pastorczak M, Kozanecki M, Ulanski J. J Phys Chem A 2008;112(43):10705–7.

[27] Walrafen GE, Hokmabadi MS, Yang W-H. J Phys Chem 1988;92:2433–8.

[28] Zhu PW, Napper DH. J Phys Chem B 1997;101:3155–60.

[29] Zhu PW, Napper DH. Macromol Chem Phys 1999;200(4):698–705.

[30] Scatena LFMGB, Richmond GL. Science 2001;292:908–12.